Volume 16 Number 14 1988 Nucleic Acids Research

Effects of macromolecular crowding on the association of *E.coli* ribosomal particles

Steven B.Zimmerman and Stefan O.Trach

Laboratory of Molecular Biology, National Institutes of Diabetes and Digestive and Kidney Diseases, National Institutes of Health, Bethesda, MD 20892, USA

Received February 24, 1988

ABSTRACT

The equilibrium for the binding reaction between the 30 S and 50 S ribosomal subunits of E. coli is shifted towards formation of 70 S ribosomes in the presence of a variety of polymers. The polymers also increase a further interaction between 70 S particles to form the 100 S dimer. The requirement for relatively high concentrations of non-specific polymers indicates that the shifts in equilibria arise from excluded volume effects. Analysis using scaled particle theory is consistent with this mechanism. The effects of high concentrations of polymers on the interactions between ribosomal species may make important changes in the function of ribosomes under the crowded conditions which occur in vivo.

INTRODUCTION

The high concentrations of macromolecules which occur in vivo can cause very large changes in rates and equilibria of cellular reactions (1,2). We have been particularly interested in effects on reactions which involve interactions between macromolecules (3-6). The association and dissociation reactions of ribosomes and their subunits (7-9) are important examples of such macromolecular interactions.

We here describe shifts in the equilibria governing association of the ribosomal subunits of E. coli to yield 70 S ribosomes (Equation 1) (10) and the further association of these 70 S ribosomes to form 100 S dimers (Equation 2) (11,12) caused by the presence of high concentrations of macromolecules.

$$30\ S + 50\ S = 70\ S \qquad \text{(Equation 1)}$$

$$2\ (70\ S) = 100\ S \qquad \text{(Equation 2)}$$

The shifts in these equilibria are shown to arise from excluded volume or macromolecular crowding effects. These results provide orientation for studies of crowding on ribosomal interactions

during protein synthesis and they also provide examples of crowding effects on defined objects of greater size than have been examined previously.

MATERIALS AND METHODS

Materials

Ribosomes. Escherichia coli D110 (pol I⁻ T⁻) was grown at 37° in LB Medium (13) containing 20 µg/ml of thymine. Cells from slowly cooled exponential phase cultures were washed with 0.15 M NaCl and stored frozen. Ribosomes were isolated from alumina extracts according to Traub et al. (14) except DNase I was omitted from the extraction buffer; aliquots of ribosomes (ca. 60 mg/ml) in 10 mM Tris·HCl, pH 7.5 - 30 mM NH_4Cl - 10 mM $MgCl_2$ - 6 mM ß-mercaptoethanol (Solution I of ref. 14) were frozen with Dry Ice and stored at -20° until used. This isolation procedure yields a mixture of 70 S and 100 S particles. Crowding effects on these ribosomes were indistinguishable from those on ribosomes isolated from E. coli C600 grown in LB medium. Ribosomes were analyzed for protein (15) using a bovine serum albumin standard, total and organic phosphorus (16), DNA (17), and A_{260} (in 25 mM Tris·HCl, pH 8.0 - 1 mM $MgCl_2$). RNA concentration was calculated from organic phosphorus concentration after correction for DNA; ribosome concentration was calculated from RNA content assuming 4566 moles P/mole of 70 S ribosomes (18). The following ranges were found in several ribosome preparations: $E^{1\%}_{260}$ = 13.8-15.8; RNA/(RNA + protein) = 53 % w/w; DNA = 1-2 % w/w.

The distribution of ribosomal species and the fraction (ca. 10%) of ribosomal units which did not aggregate at high Mg^{++} concentrations were not significantly changed by preincubation of the ribosomes under ionic conditions used elsewhere (19,20) to reactivate inactive ribosomal subunits (data not shown).

Other materials. Dextran and Ficoll samples were purchased from Pharmacia. PEG with a nominal molecular weight of 35,000 was obtained from Fluka AG, other samples of PEG were from J. T. Baker, and Coomassie Brilliant Blue G-250 was from Bio-Rad.

Methods

Assay for ribosomal subunit association. Ribosome formation and dimerization were assayed by electrophoretic separation of

HCHO-fixed (21-23) reaction mixtures. The procedure allowed rapid analysis of the equilibrium distribution of ribosomal species in large numbers of samples and in the presence of high concentrations of certain polymers. This assay is unsuited for kinetic studies because of the slow rate of HCHO-fixation.

Ribosomes were pre-equilibrated for 1 hr at 37° in 1 mM K phosphate, pH 7.7 - 50 mM KCl - 6 mM β-mercaptoethanol (21) at either 1 mM Mg acetate and 2 mg/ml of ribosomes or at 10 mM Mg acetate and 20 mg/ml of ribosomes to generate largely dissociated or largely associated ribosomal species, respectively (see following section). Reaction mixtures (40 µl total volume) contained 1 mM K phosphate buffer, pH 7.7 - 50 mM KCl - 6 mM β-mercaptoethanol - 1 mg/ml of pre-equilibrated ribosomes and the indicated concentrations of Mg acetate. Incubation was at 37° for 1 hr unless otherwise specified, followed by the addition of 2 µl of 38% formaldehyde and further incubation for 1 hr at 37°. The pH value of reaction mixtures was not significantly changed by the addition of the various polymers or control substances; mixtures after formaldehyde treatment were pH 6.9 -7.2. Samples of the pre-equilibrated ribosomes were also similarly incubated with 0.05 volume of 38% formaldehyde. The distribution of ribosomal species in formaldehyde-fixed samples was unchanged after storage for several weeks at 5° or after electrophoresis in gels containing from 1 to 10 mM Mg^{++}. Aliquots of formaldehyde-fixed reaction mixtures were mixed with an equal volume of 35% sucrose containing 0.05% bromphenol blue and 10 µl of the mixtures were applied to 1.5 mm thick 3% acrylamide-0.5% agarose gels prepared and run as described by Dahlberg *et al*. (24) except that the gel and gel buffer contained 1 mM $MgCl_2$ - 50 mM Tris·HCl, pH 8.0 and electrophoresis at 5° was for 2.5 hrs at 125 v. without buffer recirculation; gel patterns of assay mixtures were independent of the period of electrophoresis. Unless otherwise specified, gels were washed in trichloroacetic acid-methanol solution and stained with Coomassie Brilliant Blue G-250 (25). Ribosomal species were identified by gel mobilities relative to those of 16 S and 23 S RNA (24) determined on ethidium bromide stained gels.

In addition to the expected ribosomal species, smaller

amounts of an additional band (arrow in Figure 1, lane 3) appeared on the gels between the 30 S and 50 S bands . Control experiments indicate that this band partially arises during the HCHO-fixation at 37°; its appearance is accompanied by a corresponding decrease in the amount of the 50 S subunit.

Amounts of the various species were estimated from densitometer scans (Hoefer GS 300 scanning densitometer) of Coomassie Blue-stained gels. Areas of the peaks were estimated gravimetrically.

Three regions of the gel lanes were quantitated for purposes of calculation: the 70 S peak, the 100 S peak, and a combined area which includes the 30 S and 50 S peaks and the band which migrates between the 30 S and 50 S peaks (see above). The 70 S band was generally asymmetric and on some gels was partially resolved into two species with similar rates of migration and similar responses to reaction conditions; both bands were included in the area ascribed to the 70 S species. Areas were proportional to the quantity of ribosomes added to the gel for the 70 S and 100 S species individually as well as for the combined areas of the several 30 S and 50 S species.

The staining intensity of a given weight of ribosomes was not significantly affected by the state of aggregation of the ribosomes (unpublished data of the authors). Accordingly, a given area on the densitometer scan corresponds to the same number of 70 S equivalents whether that area is present as part of the combined (30 S + 50 S) area or in the 70 S or 100 S peaks. This approach assumes that there is no differential loss of subunits and, in particular, that the combined (30S + 50 S) area contains equal numbers of 30 S and 50 S particles; areas attributable to the individual species were generally in accord with this assumption. About ten per cent of the input ribosomal subunits did not aggregate under any of the conditions tested; no correction has been made for this inactive fraction. Based on the total concentration of 70 S particles added, the 70 S equivalents observed in the combined (30 S + 50 S) area and in the 70 S and 100 S peaks were converted to concentrations of the individual species.

At 37° the approach to equilibrium is sufficiently rapid to

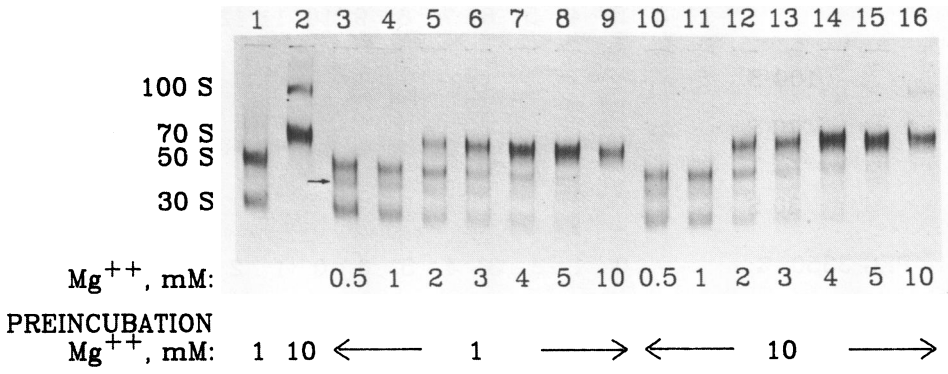

Figure 1. Effect of Mg^{++} concentration on the equilibrium distribution between ribosomal species. Ribosomes were preequilibrated at 1 or 10 mM Mg^{++} as in Methods. Samples of these preequilibration mixtures were either directly HCHO-fixed for lanes 1 or 2 or were diluted to standard assay conditions at the final Mg^{++} concentrations shown. After 1 hr at 37', aliquots were subjected to electrophoresis and stained as in Methods. The arrow indicates the additional monomer band discussed in the text. The relatively low amounts of 100 S dimer in lanes 9 and 16 vs. lane 2 reflect the lower ribosome concentration at the time of fixation with HCHO for the former samples.

set limits on the equilibrium constants in incubations of 1-4 hours. Trials at ≤ 24' did not provide useful data because of slower approach to equilibrium and greater experimental variability.

Other methods. Ribosomal RNA was isolated by phenol extraction and ethanol precipitation.

RESULTS

Effects of Mg^{++} concentration on the ribosome preparations.

The association reactions of ribosomal subunits to yield 70 S and 100 S ribosomes (Eqs. 1 and 2) are strongly dependent on Mg^{++} concentration (7,8,10,21,26); under typical dilute solution reaction conditions, i.e., non-crowded conditions, ribosomes are largely dissociated into 30 S and 50 S subunits at 1 mM Mg^{++} (Figures 1 and 2, lanes 1) and are largely associated into 70 S and 100 S particles above 10 mM Mg^{++} (Figure 1 and 2, lanes 2). The transition between ribosomal species occurs over a narrow range of Mg^{++} concentrations for the bulk of the ribosomes,

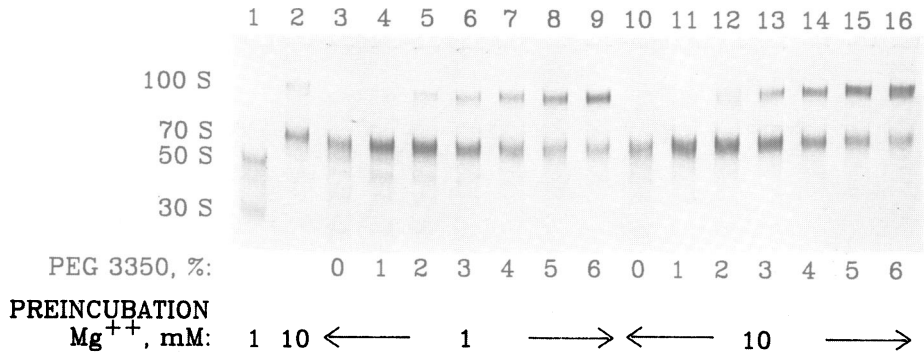

Figure 2. Effect of concentration of PEG 3350 on the equilibrium distribution between ribosomal species. Samples were prepared as for Figure 1 except that the final reaction mixtures contained 5 mM Mg^{++} and the indicated (w/v) concentrations of PEG 3350. Nominal molecular weight of PEG 3350 = 3350.

indicating limited heterogeneity in the ribosome preparation (26-28). The relatively low Mg^{++} concentration at which the transition occurs suggests the predominance of the functionally competent species ("tight vacant couples") described by Noll (29,30) that would be anticipated from the conditions during ribosome isolation.

Effects of crowding on the equilibrium positions of the association reactions.

Both the association of 30 S and 50 S subunits to form 70 S particles and the dimerization of 70 S particles to yield the 100 S species are strikingly increased by the addition of polymers. These are non-specific effects caused by a variety of polymers. A gel showing the effects of PEG 3350 is shown in Figure 2 and further data for this and other polymers are shown in Figures 3 and 4. The increases in the relative amounts of 70 S and 100 S species due to polymers are a result of shifts in the equilibrium positions of the reactions which form these species. To demonstrate this basis and to set limits on the values of the equilibrium constants under various reaction conditions, we approach equilibrium from both sides of the equilibrium position except at extreme positions of the equilibrium. Two reaction mixtures were prepared for each reaction condition to be tested

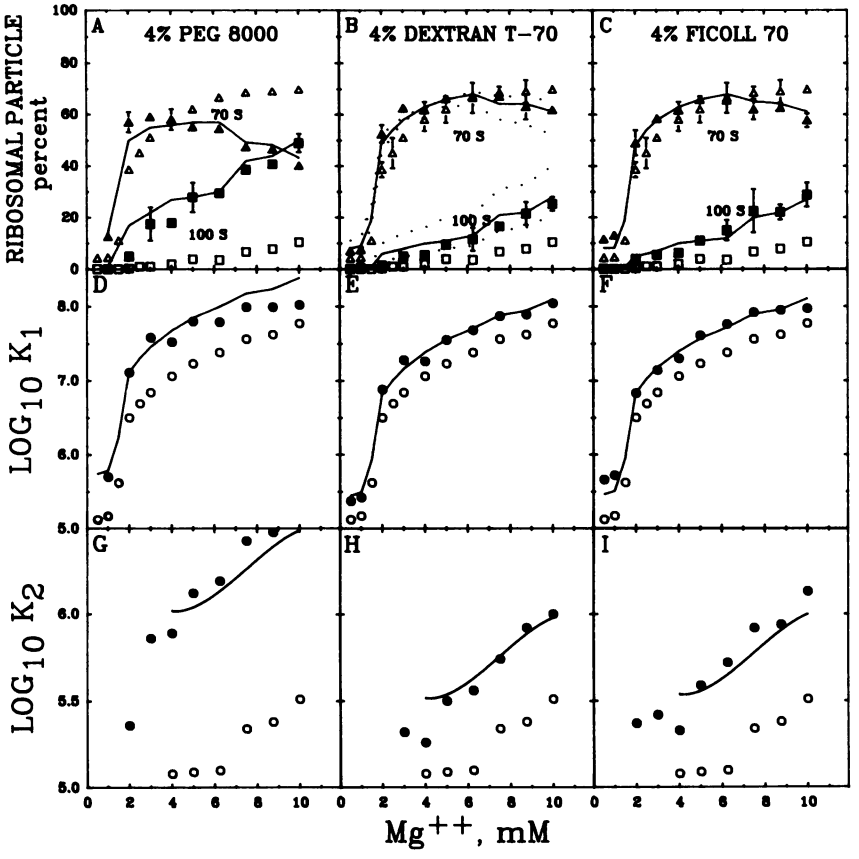

Figure 3. Effect of polymers and Mg^{++} concentration on the equilibrium distribution between ribosomal species. Open symbols, control samples; closed symbols, samples containing the indicated polymer. A-C: Amounts of 70 S (triangles) and 100 S particles (squares) are expressed as percentages by weight of the total ribosomal particles present. "Error bars" indicate the range of compositions of mixtures using ribosomes preequilibrated either at 1 or at 10 mM Mg^{++}; where not shown, the range of composition was less than the symbol size. Solid lines are theoretical values based on the theoretical values for $\log(K_1)$ and $\log(K_2)$; the theoretical value of $\log(K_2)$ at 1-3 mM Mg^{++} is assumed to be the same as that at 4 mM Mg^{++}. Dotted lines are theoretical values assuming V_A for dextran T-70 is 1/2 or twice that actually estimated. D-I: Experimental values of $\log(K_1)$ and $\log(K_2)$ that were calculated from the observed amounts of 70 S and 100 S particles in the presence of polymers (closed symbols) in A-I are compared with theoretical lines. The theoretical lines for each polymer are obtained by adding an increment, $\log(\Gamma)$, calculated as in the text, to the observed values in the absence of polymer (open symbols). Nominal molecular weight of PEG 8000 = 8000 and of dextran T-70 or Ficoll 70 = 70,000.

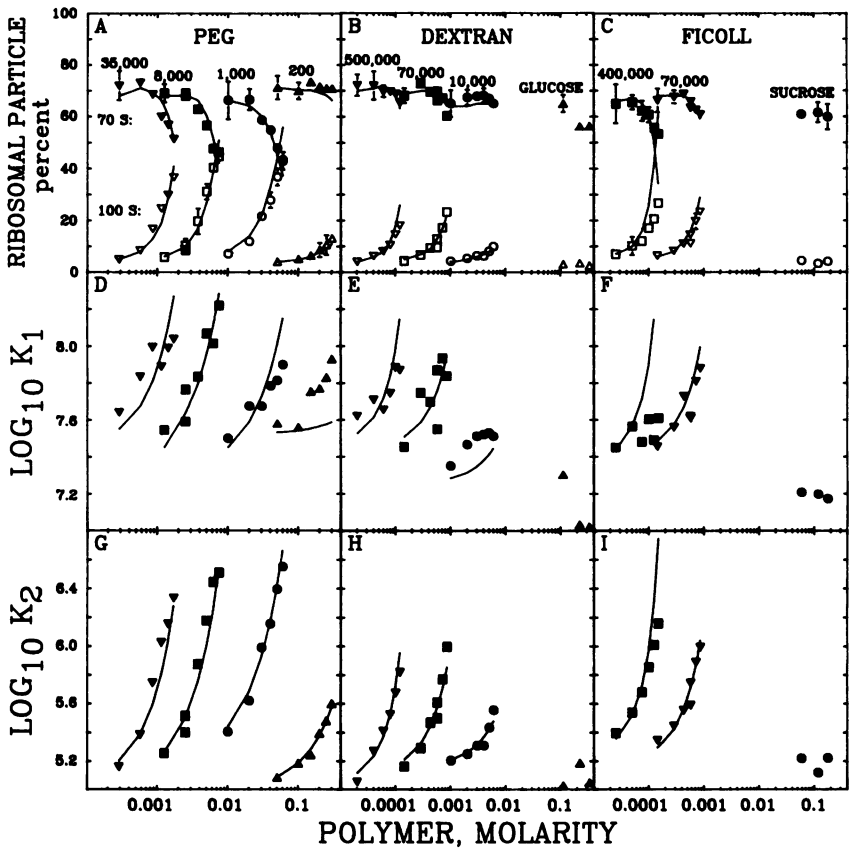

Figure 4. Effect of polymer species and molecular weight on the equilibrium distribution between ribosomal species at 5 mM Mg^{++}. The nominal average molecular weight of each polymer is shown above the data for that polymer. Observed values (symbols) are compared with theoretical values (lines). A-C: Amounts of 70 S and 100 S particles as percentages by weight of total ribosomal particles present are shown as closed and open symbols, respectively. "Error bars" used as in Figure 3.

that were identical except for the prior treatments of the ribosomes. One of each pair of mixtures contained ribosomes that had been preequilibrated at relatively high concentrations of Mg^{++} and ribosomes -- so that ca. 90% of the input ribosomes were present as 70 S and 100 S particles; the other member of the pair of mixtures had been preequilibrated at relatively low concentrations of Mg^{++} and ribosomes -- so that ca. 90% of the

input ribosomes were dissociated to 30 S and 50 S subunits. After incubation for various periods, the distribution of reaction components was fixed by addition of HCHO and analyzed as described in Methods. Examples of gels using this type of protocol are shown in Figure 1 and 2.

Data from gels similar to those in Figures 1 and 2 were used to calculate apparent concentration equilibrium constants for 70 S particle formation by equation 1 (K_1) and for dimerization of 70 S particles by equation 2 (K_2):

$$K_1 = \frac{[C_{70S}]}{[C_{30S}][C_{50S}]} \qquad K_2 = \frac{[C_{100S}]}{[C_{70S}]^2}$$

where C_i is the molar concentration of the ith species.

Values for these equilibrium constants over a range of Mg^{++} concentrations are shown in Figure 3 D-I for ribosome association in the presence (closed symbols) or absence (open symbols) of the indicated polymers. The similarity of the changes caused by PEG 8000, dextran T-70, and Ficoll 70 emphasizes the non-specific role of the polymer. In each case, addition of polymer increases the values of each equilibrium constant from those in the absence of the polymer by approximately a constant factor over a wide range of Mg^{++} concentrations. The vertical shifts between the points for the control (open symbols) and polymer samples (closed symbols) for $\log(K_1)$ and $\log(K_2)$ in Figure 3 indicate that a given polymer at a fixed concentration makes energetic contributions to the two assembly reactions that are unchanged over wide changes in concentrations of ribosomal species as well as over the conformational changes in ribososomal species which have been observed in this range of Mg^{++} concentrations (28,31,32). These shifts in equilibrium constants are consistent with a volume exclusion mechanism, representing the non-ideal contributions to the equilibrium constants due to crowding (1,2).

The results of varying the concentration of polymers at a fixed Mg^{++} concentration (5 mM Mg^{++}) are shown in Figure 4. At this Mg^{++} concentration, the bulk of the ribosomes are present as 70 S particles in the absence of polymers. Large changes in equilibrium constants are elicited by relatively low concentrations of polymers. For example, at 6% polymer (the

highest concentration shown for each polymer in Figure 4), K_1 and K_2 change by ca. 10-fold. At higher polymer concentrations still larger changes occur accompanied by higher aggregates whose identity has not been determined. The three types of polymers tested in Figure 4 are all effective in the present system at concentrations on a weight basis as much as an order of magnitude lower than those required in several other systems that are subject to crowding effects (e.g., ref. 3-6). In the following section, we show that this concentration dependence is consistent with theoretical estimates for excluded volume effects in a system in which the crowding molecules are much smaller than the reaction components.

The shifts in equilibria are strongly dependent on the molecular weight of the polymers for all three types of polymers: at the same concentration of particles, larger polymers are more effective than smaller polymers. To illustrate this point, the effects of polymers are plotted in Figure 4 vs. their nominal molarity. If, however, polymers are compared at the same concentration on a weight basis, the effects of molecular weight largely disappear, again in accord with excluded volume calculations. Finally, if the polymers are compared on the basis of the actual volume they exclude using the effective polymer volumes determined as in the Appendix, crowding effects have the expected inverse dependence on polymer molecular weight (1). Glucose and sucrose, the monomers of dextran and Ficoll, are relatively inactive and may even tend to shift K_1 towards dissociation. PEG 200, a short oligomer of polyethylene glycol, is less active than is PEG 8000 at comparable concentrations by weight.

Comparison of experimental results with scaled particle theory.

Scaled particle theory (33-36; see discussion in 1,2) has been successfully used to model excluded volume effects in several biological systems (37-39). The theory represents all the macromolecular species involved as hard particles of some arbitrary geometrical shape. Individual species are assigned different particle sizes which represent their effective volumes. Previous applications of the theory have generally dealt with compact macromolecular species such as globular proteins rather

than the relatively flexible polymers used here.

For purposes of calculation, the relative volumes of the 30 S, 50 S, 70 S and 100 S ribosomal particles were taken to be 0.375, 0.625, 1 and 2, respectively. These relative volumes for the 30 S, 50 S and 70 S species are based on experimental values determined by a variety of techniques (7); they are consistent with the molecular weights of the respective species (ca. 1.0×10^6, 1.7×10^6 and 2.7×10^6 for 30 S, 50 S and 70 S particles, respectively). The 100 S dimer is assumed to have a volume twice that of the 70 S particle. The absolute volume of the 70 S particle is taken as 4.0×10^{-18} cm^3 (7; see also Appendix). Equation A3 of reference 40 was used to calculate the contribution of crowding to the chemical potential of each ribosomal particle involved in the equilibria. These contributions were then combined in accord with the stoichiometry of Equations 1 or 2 to give the non-ideal contributions due to crowding for the respective equilibrium constants, K_1 or K_2. We compare calculations assuming either cubical or spherical shapes for both the ribosomal particles and the molecules used to crowd the solution in the Appendix.

The effective particle volume which each polymer displayed was determined from the observed shift in K_2 as described in the Appendix. A single effective particle volume served for each polymer preparation over the range of polymer concentrations analyzed (1 to 6 %), indicating that the polymers can be adequately modeled as effective hard particles of fixed volume. Values calculated from scaled particle theory are shown as solid lines which can be compared with the experimental data in the presence of polymers (closed symbols) in Figures 3 for the Mg^{++} concentration dependence and with both the open and closed symbols in Figure 4 for the polymer concentration and polymer molecular weight dependences. Effective polymer volumes are estimated to have an uncertainty of $\leq$ 2-fold; the effects of a 2-fold variation in volume are illustrated by the dotted lines in Figure 3B.

The effective particle volume for each polymer is derived from the experimental variation in K_2 as a function of polymer concentration; theoretical values for $\log(K_2)$ based on these

effective volumes (solid lines in Figure 4 G-I) agree with the experimental changes observed in $\log(K_2)$ (filled symbols in Figure 4 G-I). It is highly significant that calculations using these volumes also agree relatively well with the experimental variations in $\log(K_1)$ under a variety of conditions (solid lines vs. filled symbols in Figure 3 D-F and Figure 4 D-F) as well as with the observed proportions of 70 S and 100 S particles (solid lines vs. filled symbols in Figure 3 A-C and solid lines vs. both the open symbols (100 S particles) and filled symbols (70 S particles) in Figure 4 A-C). This ability of effective volumes inferred from variation in K_2 to predict changes in both K_1 and K_2 is fully consistent with a common mechanism, volume exclusion, being responsible for the effects on both equilibria.

DISCUSSION

A number of lines of evidence indicate that polymers affect the equilibria of the reactions forming 70 S and 100 S particles due to the volume exclusion properties of the polymers. The lack of specificity with regard to the polymer and the inactivity of the corresponding monomers are qualitatively consistent with such a mechanism. In addition, theoretical calculations for this mechanism fit the observed dependences on polymer concentration and polymer molecular weight. For these reasons, we conclude that changes in amounts of the various ribosomal species in the presence of the crowding polymers are a direct result of excluded volume effects. Are such effects likely to be of importance in the functioning of living cells?

Under growth conditions in E. coli, ribosome subunit association is part of a cycle (41): the 30 S ribosomal subunit and mRNA first form a complex. The 50 S ribosomal subunit adds to this complex to yield a functional 70 S ribosome-mRNA complex which sequentially translates the mRNA. Upon completion of translation, the ribosome dissociates from the message to once more generate 30 S and 50 S subunits. Among the variety of factors which participate in this cycle is one which aids in the dissociation of the 70 S particles. Early studies (21,42) raised the question of the role of such a factor, since it appeared from these studies that dissociation might be a spontaneous

process. More recent measurements with "tightly coupled" ribosomes indicate, however, that under physiological ionic conditions (but in uncrowded media), some cellular mechanism of ribosome dissociation is probably required (26). Our results suggest that the need for an efficient mechanism of dissociation is much greater than had been previously estimated because of the tendency towards association due to the crowded nature of the cytoplasm. It would be of considerable interest to extend studies of crowding to systems of increasing complexity which can carry out increasing parts of the overall process of protein synthesis. It is anticipated that the binding reactions of the other macromolecules involved in protein synthesis (tRNA species, mRNA, protein factors) and perhaps even the stoichiometry of the proteins of the ribosome itself will be significantly affected by excluded volume effects (28,43).

The equilibria expressed in Equations 1 and 2 are remarkably sensitive to exogenous polymers. It is interesting to consider the increase in total ribosome concentration that would be necessary to cause the same shifts in equilibria. For example, it would require approximately a three-fold increase in total ribosome concentration to obtain the shifts in equilibria of Figure 3 that were caused by the addition of 4% polymer. The much larger shifts which can be obtained at higher concentrations of polymers (Figure 4 and unpublished data of the authors) would require yet higher and perhaps experimentally intractable concentrations of ribosomes in the absence of polymers.

Finally, we comment on another way of affecting the equilibria between ribosome species which is also dependent on volume changes in the reactions but which has a quite different origin. Changes in hydrostatic pressure have been shown to cause shifts in ribosomal association (44-46); increased pressure favors the dissociation of ribosomes. Such pressure effects as well as the crowding effects that we have shown are both responses to the molecular volumes of the participants of the reaction (47-51). The differences between the two types of effects can be considered in terms of contributions to the free energy change of the reaction (Equation 3). For a reversible

reaction at constant temperature (52):

$$(dG)_T = PdV + \Sigma_i (\mu_i\, dn_i) \qquad \text{(Equation 3)}$$

where $(dG)_T$ is the change in Gibbs free energy at a fixed temperature as a function of the pressure (P), volume change of the reaction (dV), and the chemical potentials (μ_i) and number of moles (n_i) for the ith species. Pressure affects the magnitude of the PdV term; from ultracentrifugation experiments, the formation of 70 S particles by equation 1 is calculated to have a volume increase of the order of 0.01 %. As the hydrostatic pressure is increased, the 70 S particles tend to dissociate to minimize the total volume requirement. In contrast, crowding effects do not require a net change in the volume for the reaction (1,2); the theoretical lines for crowding effects in Figures 3 and 4 are calculated assuming no net change in volume for either association reaction. Changes in the values of the equilibrium constants due to crowding arise because the chemical potentials of the various ribosomal particles involved in the equilibria are changed to different extents by crowding depending on their volumes and shapes -- reflecting the frequency with which "free" volumes can be found in the solution to accommodate each species of particle. It is the resultant for the overall reaction of these changes in chemical potentials (second term of Eq. 3) which is the energetic contribution of crowding to the reaction .

ACKNOWLEGEMENT

The comments of Gary Felsenfeld, Martin Gellert, Allen Minton and Philip Ross are very much appreciated.

ABBREVIATIONS

PEG, polyethylene glycol; V_A, effective molecular volume of polymer additive; $V_{70\,S}$, particle volume of the 70 S ribosome; M_A, nominal average molecular weight of polymer additive; $M_{70\,S}$, molecular weight of the 70 S ribosome.

REFERENCES

1. Minton, A.P. (1981) Biopolymers 20, 2093-2120.
2. Minton, A.P. (1983) Molec. Cell. Biochem. 55, 119-140.

3. Zimmerman, S.B. and Pheiffer, B. (1983) Proc. Natl. Acad. Sci. USA 80, 5852-5856.
4. Harrison, B. and Zimmerman, S.B. (1986) Nucleic Acids Res. 14, 1863-1870.
5. Zimmerman, S.B. and Harrison, B. (1987) Proc. Natl. Acad. Sci. USA 84, 1871-1875.
6. Zimmerman, S.B. and Trach, S.O. (1988) Biochim. Biophys. Acta, in press.
7. Van Holde, K.E. and Hill, W.E. (1973) in Nomura, Y., Tissières, A. and Lengyel, P. (eds.) Ribosomes, Cold Spring Harbor, New York, pp.53-91.
8. Spirin, A.S. (1986) Ribosome Structure and Protein Biosynthesis, Benjamin/Cummings, Menlo Park.
9. Oakes, M., Henderson, E., Scheinman, A., Clark, M. and Lake, J.A. (1986) in Hardesty, B. and Kramer, G. (eds.) Structure, Function, and Genetics of Ribosomes, Springer-Verlag, New York, pp. 47-66.
10. Tissières, A., Watson, J.D., Schlessinger, D. and Hollingworth, B.R. (1959) J. Mol. Biol. 1, 221-233.
11. Tissières, A. and Watson, J.D. (1958) Nature 182, 778-780.
12. Bernabeu, C. and Lake, J.A. (1982) J. Mol. Biol. 160, 369-373.
13. Maniatis, T., Fritsch, E.F. and Sambrook, J. (1982) Molecular Cloning, Cold Spring Harbor Laboratory, New York, p.68.
14. Traub, P., Mizushima, S., Lowry, C.V. and Nomura, M. (1971) in Moldave, K. and Grossman, L. (eds.) Methods in Enzymology, Vol. 20, Part C, Academic Press, New York, pp. 392-393.
15. Lowry, O.H., Rosebrough, N.J., Farr, A.L. and Randall, R.J. (1951) J. Biol. Chem. 193, 265-275.
16. Ames, B.N. and Dubin, D.T. (1960) J. Biol. Chem. 235, 769-775.
17. Ashwell, G. (1957) in Colowick, S.P. and Kaplan, N.O. (eds.), Methods in Enzymology, Vol. 3, Academic Press, New York, pp. 99-101.
18. Noller, H.F. (1984) Ann. Rev. Biochem. 53, 119-162.
19. Miskin, R., Zamir, A. and Elson, D. (1970) J. Mol. Biol. 54, 355-378.
20. Zamir, A., Miskin, R. and Elson, D. (1971) J. Mol. Biol. 60, 347-364.
21. Zitomer, R.S. and Flaks, J.G. (1972) J. Mol. Biol. 71, 263-279.
22. Moore, P.B. (1966) J. Mol. Biol. 22, 145-163.
23. Spirin, A.S., Sofronova, M.Y. and Sabo, B. (1970) Molec. Biol. 4, 501-508.
24. Dahlberg, A.E., Dingman, C.W. and Peacock, A.C. (1969) J. Mol. Biol. 41, 139-147.
25. Blakesly, R.W. and Boezi, J.A. (1977) Anal. Biochem. 82, 580-582.
26. Noll, M. and Noll, H. (1976) J. Mol. Biol. 105, 111-130.
27. Debey, P., Hui Bon Hoa, G., Douzou, P., Godefroy-Colburn, T., Graffe, M. and Grunberg-Manago, M. (1975) Biochemistry 14, 1553-1559.
28. Spitnik-Elson, P. and Elson, D. (1976) Prog. Nucleic Acids Res. Mol. Biol. 17, 77-98.
29. Noll, M., Hapke, B. and Noll, H. (1973) J. Mol. Biol. 80, 519-529.
30. Hapke, B. and Noll, H. (1976) J. Mol. Biol. 105, 97-109.

31.Ghysen, A., Bollen, A. and Herzog, A. (1970) Eur. J. Biochem. 13, 132-136.
32.Van Duin, J., van Dieijen, G., van Knippenberg, P.H. and Bosch, L. (1970) Eur. J. Biochem. 17, 433-440.
33.Reiss, H., Frisch, H.L., Helfand, E. and Lebowitz, J.L. (1960) J. Chem. Phys. 32, 119-124.
34.Lebowitz, J.L., Helfand, E. and Praestgaard, E. (1965) J. Chem. Phys. 43, 774-779.
35.Gibbons, R.M. (1969) Molecular Physics 17, 81-86.
36.Gibbons, R.M. (1970) Molecular Physics 18, 809-816.
37.Ross, P.D. and Minton, A.P. (1977) J. Mol. Biol. 112, 437-452.
38.Ross, P.D. and Minton, A.P. (1979) Biochem. Biophys. Res. Commun. 88, 1308-1314.
39.Minton, A.P. and Wilf, J. (1981) Biochemistry 20, 4821-4826.
40.Chatelier, R.C. and Minton, A.P. (1987) Biopolymers 26, 507-524.
41.Watson, J.D., Hopkins, N.H., Roberts, J.W., Steitz, J.A. and Weiner, A.M. (1987) Molecular Biology of the Gene, Vol. I, 4th edn., pp. 382-430, Benjamin/Cummings, Menlo Park.
42.Sabo, B. and Spirin, A.S. (1970) Molecular Biol. 4, 509-511.
43.Liljas, A. (1982) Prog. Biophys. Molec. Biol. 40, 161-228.
44.Infante, A.A. and Krauss, M. (1971) Biochim. Biophys. Acta 246, 81-99.
45.Infante, A.A. and Baierlein, R. (1971) Proc. Natl. Acad. Sci. USA 68, 1780-1785.
46.Van Diggelen, O.P., Oostrom, H. and Bosch, L. (1971) FEBS Letters 19, 115-120.
47.Jaenicke, R. (1981) Ann. Rev. Biophys. Bioeng. 10, 1-67.
48.Weber, G. and Drickamer, H.G. (1983) Quart. Rev. Biophysics 16, 89-112.
49.Kegeles, G., Rhodes, L. and Bethune, J.L. (1967) Proc. Natl. Acad. Sci. USA 58, 45-51.
50.TenEyck, L.F. and Kauzmann, W. (1967) Proc. Natl. Acad. Sci. USA 58, 888-894.
51.Josephs, R. and Harrington, W.F. (1967) Proc. Natl. Acad. Sci. USA 58, 1587-1594.
52.Daniels, F. and Alberty, R.A. (1966) Physical Chemistry, 3rd edn., p. 105, Wiley, New York.
53.Tanford, C. (1961) Physical Chemistry of Macromolecules, pp. 150-170, Wiley, New York.

APPENDIX

ESTIMATION OF EFFECTIVE VOLUMES OF POLYMERS

In order to use scaled particle theory to calculate shifts in equilibrium, we assume that the polymer used to crowd the ribosomes as well as the ribosomes themselves can be represented as effective hard particles of unique size. It was not clear whether flexible polymers would behave in such a fashion over a useful range of polymer concentrations (2). Accordingly, for each concentration of interest, the shift in K_2 (expressed as $\log(\Gamma_{K2})$ where Γ is the non-ideal contribution to K_2 due to

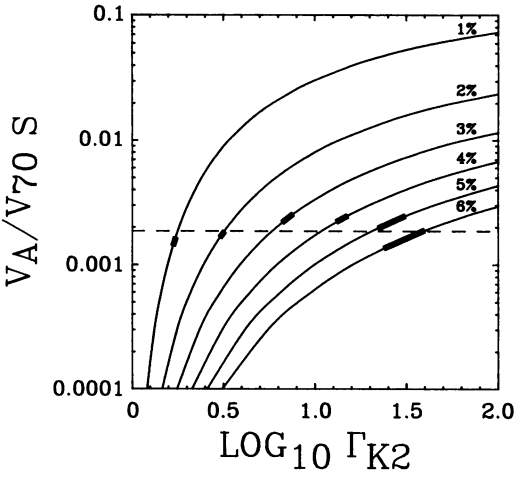

Appendix Figure 1. Effective volume of PEG 8000 inferred from observed shifts in the equilibrium constant for 70 S dimerization. Curves are calculated for the indicated concentrations of PEG 8000 (% w/v) as described in text. The experimental ranges of shifts in the observed equilibrium distributions in $\log(K_2)$, i.e. $\log \Gamma_{K2}$, are indicated by the heavy lines. The value of $V_A/V_{70\ s}$ inferred is indicated by the dashed line.

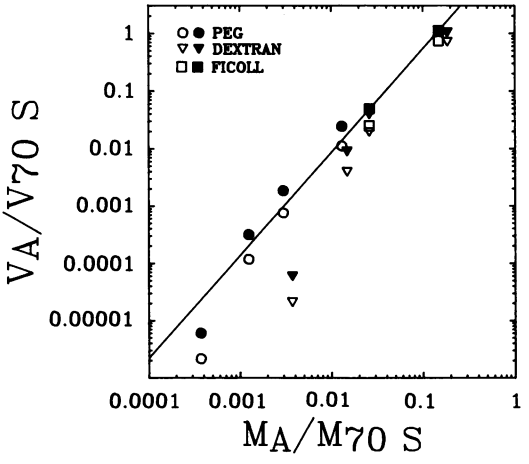

Appendix Figure 2. Molecular weight dependence of the polymer volumes inferred from polymer effects on the 70 S dimerization reaction. Open and closed symbols indicate cubical and spherical models, respectively. Molecular weight (M_A) and volume (V_A) of each polymer are expressed relative to those of the 70 S particle ($M_{70\ s}$ and $V_{70\ s}$). The line indicates a slope of 1.8 (see text).

crowding) (1,2) was calculated as a function of the volume of the effective hard sphere, V_A (expressed as a fraction of the volume of the 70 S particle, V_A/V_{70S}). Appendix Figure 1 shows such a calculation for 1 to 6 % PEG 8000. The experimentally observed shifts in $\log(K_2)$ are indicated by the heavy portions of the lines. Similar calculations were done for all the polymers tested in Figure 4.

Do these volumes have the characteristic molecular weight dependence expected for flexible polymers (53)? For the present approximate analysis, we assume each polymer is a homogeneous population with a molecular weight equal to the nominal average molecular weight. For ideal flexible polymers, the radius of gyration should increase with (molecular weight)$^{0.5-0.6}$, so that the corresponding volume should increase as (molecular weight)$^{1.5-1.5}$. If the polymer is too short to behave as a random coil, it will appear stiffer and have a volume dependence on (molecular weight)$^{1.8-3.0}$. When analyzed in this fashion, most of the samples of polymers tested have a dependence close to (molecular weight)$^{1.8}$ (line in Appendix Figure 2) as expected for large flexible polymers. The smallest dextran and the smallest polyethylene glycol preparations tested had effective volumes which suggested either a size-dependent stiffness or perhaps an ability to penetrate into parts of the ribosomal species which are unavailable to the larger polymers.

The preceding calculations have assumed a spherical shape for the ribosomal species as well as the polymers. The effect of choosing a cubical model of the same volume is indicated by the open symbols in Appendix Figure 2 as compared to the closed symbols for the spherical model. A value for the volume of the 70 S particle is assumed for purposes of this analysis. There is a range of about two-fold in the experimental estimates of this value for the 70 S particle; that range corresponds for spherical particles to about the amount of difference in V_A/V_{70S} between the open and closed symbols in Appendix Figure 2.